

Clustering of solitons in weakly correlated wavefronts

Zhigang Chen^{*†}, Suzanne M. Sears^{*§}, Hector Martin[†], Demetrios N. Christodoulides[‡], and Mordechai Segev^{*§¶}

^{*}Physics Department and Solid State Institute, Technion, Haifa 32000, Israel; [†]Department of Physics and Astronomy, San Francisco State University, San Francisco, CA 94132; [‡]Electrical Engineering and Computer Science Department, Lehigh University, Bethlehem, PA 18015; and [§]Princeton University, Princeton, NJ 08544

Edited by Martin D. Kruskal, State University of New Jersey–New Brunswick, Piscataway, NJ, and approved November 29, 2001 (received for review June 6, 2001)

We demonstrate theoretically and experimentally the spontaneous clustering of solitons in partially coherent wavefronts during the final stages of pattern formation initiated by modulation instability and noise.

Clustering, or the gross-scale aggregation of fine-scale structures, has been observed in many diverse physical systems: from galactic clusters (1, 2) to molecular aggregates (3, 4), from self-assembled quantum dots (5) to biological systems (6), just to name a few. Despite the great variety of physical systems in which these clustering phenomena occur, the underlying processes are fundamentally similar in several ways. This similarity is actually a manifestation of two characteristic features: (i) the fine structure results from the equilibrium of opposing effects or forces, and (ii) the cluster forms because of attraction between these individual “fine-scale elements.” For example, a protein molecule may be made up by more than one polypeptide chain. In the case of hemoglobin, four separate polypeptide chains, or subunits, are clustered together (held together by van der Waals and ionic forces). In astrophysics, gravitational attraction is known to lead to the formation of galaxies and galactic clusters. Given the universality of these processes, one may be able to study clustering of fine-scale elements in a number of completely different physical systems. In fact, propositions were recently made to use Bose–Einstein condensates to simulate galactic environments (7, 8). It would be very interesting if similar dynamics, namely, the clustering of fine-scale elements, could be observed in optical settings where the ensemble interaction forces can be varied at will and the underlying theory is well understood.

Here we report the experimental observation of clustering of optical solitons. The clustering of solitons occurs spontaneously, when a partially incoherent optical wavefront disintegrates in a noninstantaneous nonlinear medium with a large enough self-focusing nonlinearity. This process is initiated by noise-driven modulation instability (MI), which in turn leads to the formation of soliton-like self-trapped filaments. These solitonic filaments tend to attract one another, eventually leading to the formation of clusters of solitons. The incoherence of the wavefront (which can be varied in a controlled manner), along with the noninstantaneous nature of the nonlinearity, give rise to attractive forces between the solitonic filaments involved. The experimental results are in agreement with theoretical predictions and are confirmed by using numerical simulations.

To further elaborate on these ideas, we introduce some aspects of solitons, and in particular, the ideas underlying incoherent or random-phase solitons. Other relevant topics, such as those pertaining to the recent discoveries of MI and pattern formation in incoherent (or weakly correlated) nonlinear wave systems, will also be discussed.

Solitons are stationary localized wavepackets that travel “without change of shape or diminution of speed” in dispersive nonlinear wave systems.[¶] Here we use the term soliton to denote any solitary wavepacket, i.e., in the broader definition of the word that includes self-trapped solutions of nonintegrable systems (9). Solitons share many features with real particles: for example, their total energy and momentum are conserved even

when they interact with one another. In addition, solitons retain their shape and identity after a collision event. Thus far, solitons have been predicted and their existence has been demonstrated in many physical systems. Such examples include surface solitary waves in shallow water,^{||} plasma solitons (10), sound waves in ³He (11), short temporal soliton pulses in fibers (12, 13), and optical spatial solitons (14–17). Despite this diversity, the main principles behind soliton formation and soliton interactions are the same. Intuitively, solitons form when the broadening tendency of diffraction (or dispersion) is balanced by nonlinear self-focusing. Until 1990, most research on optical solitons concentrated on trapping in a single dimension. Examples of such one-dimensional self-trapped wavepackets are temporal fiber solitons (12) and spatial solitons (18) in slab waveguides. In general two-dimensional (2D) bright solitons in Kerr media are known to be highly unstable and undergo catastrophic collapse (19, 20). However, in the past decade, major progress has been made with solitons in saturable nonlinear media where stable solitons of higher dimensionality can be generated. These include 2D spatial solitons in bulk media (17), spatio-temporal solitons that can be self-trapped in one dimension in space and time (21), and even “optical bullets” that are self-trapped in both transverse spatial dimensions and time simultaneously.^{**} This general view of solitons being the result of a balance between diffraction/dispersion and self-focusing also holds in all of these cases of a higher dimensionality provided that the wavepacket exhibits stable self-trapped propagation. Another way to understand soliton formation comes from the so-called self-consistency principle: this idea implies that a soliton forms when a localized wavepacket induces (by the nonlinearity) a waveguide and in turn is “captured” in it, thus becoming a bound state in its own induced potential (22). In the spatial domain of optics, a soliton results when a very narrow optical beam induces, by self-focusing, a waveguide structure and guides itself in it. Thus, interactions (collisions) between solitons can be viewed as interactions between bound states of a jointly induced potential well, or between bound states of different wells located at close proximity (17). In nonintegrable systems (such as those with saturable nonlinearities), interactions between solitons exhibit very rich behavior compared with those in integrable systems (17).

Relevant to our discussion is the class of incoherent solitons. For decades, solitons were believed to be solely coherent entities. This perception changed, however, just a few years ago, when partially spatially incoherent solitons were first observed in 1996 (23). Observations of temporally and spatially incoherent (“white”) light solitons (24) followed soon thereafter. These

This paper was submitted directly (Track II) to the PNAS office.

Abbreviations: MI, modulation instability; 2D, two-dimensional.

[¶]To whom reprint requests should be addressed. E-mail: msegev@tx.technion.ac.il.

^{||}Russell, J. S., 14th meeting of the British Association for the Advancement of Science, 1844, London.

^{**}Di Trapani, P., Workshop on Optical Solitons, March 23–24, 2001, Orlando, FL.

The publication costs of this article were defrayed in part by page charge payment. This article must therefore be hereby marked “advertisement” in accordance with 18 U.S.C. §1734 solely to indicate this fact.

experiments proved that indeed solitons made of random-phase (or incoherent) wavepackets can exist. As a result, entirely new directions in soliton science have opened up. Shortly thereafter, the theory of incoherent solitons was developed (25–30) and dark incoherent solitons were observed (31). Further studies considered their interactions (32), their stability properties (33), and their relation to multimode composite solitons (34). Crucial to the existence of incoherent solitons is the noninstantaneous nature of the nonlinearity, which responds only to the time-averaged intensity structure of the beam, rather than to the instantaneous, highly speckled, and fragmented wavefront. In other words, the response time of the nonlinear medium must be much longer than the average time of phase fluctuations across the beam. Through the nonlinearity, the time-averaged intensity induces a multimode waveguide structure (a potential well that can bind many states), whose guided modes are populated by the optical field with its instantaneous speckled structure.

Central to our discussion is the concept of MI and its occurrence in random-phase (or incoherent) systems. MI is a universal process that appears in most nonlinear wave systems in nature. MI causes small amplitude and phase perturbations (from noise) to grow rapidly under the combined effects of nonlinearity and dispersion/diffraction. As a result, uniform excitations (such as broad optical beams in the spatial domain in optics or very long pulses in the temporal domain) tend to disintegrate during propagation (35–45), leading to filamentation or break-up into pulse trains. The relation between MI and solitons is best illustrated by the fact that the filaments (or the pulse trains) that emerge from the MI process are actually trains of almost ideal solitons. MI therefore can be considered as a precursor to soliton formation. [Interestingly, this view also holds for the breakup of one-dimensional solitons in bulk media, the so-called transverse instability, which leads to the breakup of a one-dimensional beam into an array of 2D filaments. In Kerr media, 2D beams are unstable, so the entire structure is unstable and the whole beam quickly disintegrates (see ref. 46). However, in saturable nonlinear media, such an array of 2D filaments is stable and is in fact an array of 2D solitons (see, e.g., ref. 47).] Over the years, MI has been systematically investigated in connection with numerous nonlinear processes; yet it was always believed that MI is inherently a coherent process and can appear only in nonlinear systems with a perfect degree of spatial/temporal coherence. Recent theoretical and experimental studies (48, 49) have shown that MI can also occur in partially incoherent (or random phase) wavefronts and have demonstrated that, even in such a system of weakly correlated “particles,” patterns can form spontaneously. However, such incoherent MI appears only if the strength of the nonlinearity exceeds a well-defined threshold that depends on the coherence properties (correlation distance) of the wavefront. The discovery of incoherent MI has implications for many other nonlinear systems beyond optics. It implies that patterns can form spontaneously (from noise) in nonlinear many-body systems involving weakly correlated particles, such as, for example, atomic gases at (or slightly above) the Bose–Einstein–condensation temperatures (49).

In light of the above, one may wonder how the solitonic filaments emerging from the MI and breakup of a partially coherent yet uniform wavefront ultimately will behave. In fully coherent systems with saturable nonlinearities, such solitary filaments are stable and interact in the same manner as solitons: they may either attract or repel one another, depending on their relative phase. As a result, the filaments arising from MI in coherent (saturable) systems do not cluster together; instead, the presence of repulsive forces leads to almost evenly spaced solitons in a quasi-ordered lattice structure. If the underlying nonlinearity is of the Kerr type, then the products of transverse instability are 2D filaments that are

highly unstable and tend to disintegrate, and thereby cannot form such a structure. On the other hand, in incoherent self-focusing systems soliton interactions over scales larger than the correlation length are always attractive. [See review on soliton interactions in ref. 17. The interaction forces between solitons in such systems were first studied theoretically in ref. 50. The first experimental demonstration of incoherent interaction between solitons was reported in refs. 51 and 52.] Such an incoherent interaction is always attractive because the relative phase between adjacent solitons varies much faster than the response time of the nonlinear medium (recall that the noninstantaneous nature of the nonlinearity is a prerequisite for the formation of incoherent solitons and incoherent MI). When two incoherent solitons are brought to close proximity, their intensities add in the center region between them, leading to an increase in the refractive index. This process, in turn, attracts more light to the center, moving the centroid of each soliton toward it and hence the solitons appear to attract one another (17).

Results

To analyze this process theoretically we use the coherent density approach (25, 26) that describes the propagation dynamics of partially spatially incoherent (quasi-monochromatic) optical beams in noninstantaneous nonlinear media. For the propagation medium, we choose a saturable nonlinearity of the type

$$\Delta n(I) = \frac{\Delta n_0 I / I_s}{(1 + I / I_s)}$$

where Δn is the nonlinear change in the refractive index as a function of the total intensity I , Δn_0 is the maximum change in the refractive index, and I_s is the saturation intensity (a constant factor indicating the degree of saturation). This specific form of nonlinearity represents the true nonlinear response of a homogeneously broadened two-level system at the vicinity of an electronic transition, and, to a reasonable approximation, it also represents the photorefractive screening nonlinearity (53–55). We study clustering in a $(2 + 1)$ dimensional system, in which the optical beam propagates along the z -direction and undergoes diffraction or self-trapping in two transverse (x and y) dimensions. In such a system it is essential to use a saturable nonlinearity (e.g., the nonlinearity used in our experiment). Otherwise, all self-focusing effects that start from a beam with power exceeding a particular value (the critical power), lead to catastrophic collapse, in which the self-focusing processes never stabilize into a 2D filament (19, 20).

In the coherent density approach, the propagation of incoherent light in slow-responding nonlinear media (such as biased photorefractive crystals) is described by superimposing infinitely many “coherent components” or quasi-particles all interacting by means of the nonlinearity. In this picture the initial relative weights of these components are given by the angular power spectrum of the source beam, which is physically the Fourier transform of the correlation function. Mathematically this is modeled by using the coherent density function, f , from which one can obtain both the intensity and the correlation function of a partially coherent beam during propagation. The coherent density function is governed by the following integro-differential equation (25, 26):

$$i \left(\frac{\partial f}{\partial z} + \theta_x \frac{\partial f}{\partial x} + \theta_y \frac{\partial f}{\partial y} \right) + \frac{1}{2k} \left(\frac{\partial^2 f}{\partial x^2} + \frac{\partial^2 f}{\partial y^2} \right) + k_{\text{eff}} g(I_N(x, y, z)) f = 0,$$

where

$$I_N = \iint |f(x, y, z, \theta_x, \theta_y)|^2 d\theta_x d\theta_y,$$

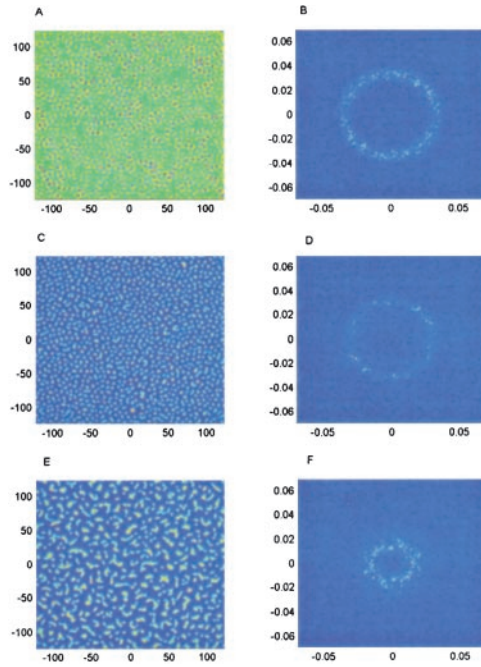


Fig. 1. Numerical simulation of propagation of partially coherent wavepacket in saturable nonlinear media. (A) The growth of perturbations after 1 mm of propagation and (B) its Fourier transform. (C) The development of individual solitons at 2 mm and (D) its Fourier transform. After 3 mm, clustering develops (E); (F) its Fourier transform. The vertical and horizontal scales are micrometers in A, C, and E and radians in B, D, and F.

and, at $z = 0$,

$$f(z = 0, x, y, \theta_x, \theta_y) = G_N^{1/2}(\theta_x, \theta_y)\phi_o(x, y).$$

In the equation above, θ_x and θ_y are angles (in radians) with respect to the z axis, $k = k_o n_o$, and $k_o = 2\pi/\lambda_o$. The function $f(x, y, z, \theta_x, \theta_y)$ is a band-limited function and is of negligible amplitude outside of the narrow paraxial angular range. Thus, even though the integration is formally over all transverse momentum space, i.e., k space, the only contributing range is an angular range of $\approx \pm 0.1$ radians. $G_N(\theta_x, \theta_y)$ is the normalized angular power spectrum of the incoherent source, and $\phi_o(x, y)$ is the wavefront's input spatial modulation function. $I_N = I/I_s$ and $g[I_N(x, y, z)]$ represents the intensity dependence of the nonlinearity given by $n^2 = n_o^2 + 2n_o g(I_N)$. As previously mentioned, here the nonlinearity is taken to be of the form $g(I_N) = \Delta n_o I_N / (1 + I_N)$ (saturable nonlinearity). In our simulations the linear index is $n_o = 2.3$, and the maximum nonlinear index change is taken to be $\Delta n_o = 2.5 \times 10^{-3}$ (which is roughly the maximum attainable index change in inorganic photorefractive crystals). The wavelength of the light source is $\lambda_o = 0.488 \mu\text{m}$, and thus $k = 29.613 \mu\text{m}^{-1}$, and $k_o = 12.875 \mu\text{m}^{-1}$. The angular power spectrum is assumed to be of the Gaussian type $G_N(\theta_x, \theta_y) = 1/(\pi\theta_o^2) \exp(-(\theta_x^2 + \theta_y^2)/\theta_o^2)$ and $\phi_o(x, y)$ is taken to be a very broad, yet finite, flat wavefront ($\phi_o(x, y) = \exp[-(x^2 + y^2)^m / 2W_o^{2m}]$, where $m = 4$ and $W_o = 500 \mu\text{m}$).

The pictures in Fig. 1 show the results of numerical simulations carried out at an intensity ratio $I_N = 1$ in normalized units, seeded with random Gaussian white noise^{††} at a level of 10^{-5} .

^{††}White noise was added in the frequency domain by adding a random number chosen from a Gaussian distribution separately to both the real and imaginary parts of each Fourier component. The width of the Gaussian distribution was chosen so that the average power added by the noise would be some small fraction of the total power, in our case 10^{-5} .

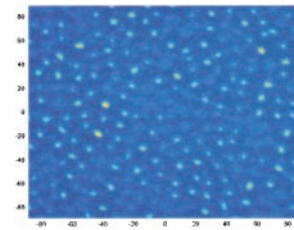


Fig. 2. Simulation of coherent wavefronts in nonlinear media after 3 mm of propagation. Shown is the (output) intensity pattern displaying multiple evenly spaced solitonic filaments. The vertical and horizontal scales are micrometers.

Fig. 1 A, C, and E depicts the intensity of the partially coherent wavefront whereas Fig. 1 B, D, and F shows the 2D Fourier transform of the intensity pattern. The input to the system was a partially incoherent spatially initial uniform broad beam. The width of the initial angular power spectrum θ_o is assumed to be 13.85 millirads, which corresponds to an initial correlation length of $6.3 \mu\text{m}$. In Fig. 1A, we see as expected, that perturbations of certain spatial frequencies are favored by the MI process and have begun to grow on top of the input (48, 49); Fig. 1B shows that these frequencies are contained within a rather narrow ring. As the propagation continues, the ripples grow stronger until the beam disintegrates into solitary filaments (Fig. 1C), indicating a balance between the effects of diffraction and nonlinearity. Interestingly enough, little has changed in the frequency domain (Fig. 1D); there is still a single thin ring of a well-defined radius. This radius or spatial frequency is in fact related to average distance between solitary filaments (or particles), which is fairly uniform. Now, however, the particle-like nature of the solitons starts to affect the overall dynamics of the partially coherent system, signaling the onset of a qualitatively new stage of behavior. As discussed above, in incoherent systems, only attractive forces between the solitary filaments (particles) need be considered for separation distances longer than the correlation length. Thus, as small random movements accidentally bring two solitons closer together, the mutual potential well caused by their joint overlapping intensities will further strengthen the attractive force between them. As a result, the peaks will be drawn toward one another. What ensues is best described as clustering; the interplay of the forces among particles eventually leads to the grouping of quasi-particles with their nearest neighbors (see Fig. 1E). The overall size of each of the clusters continues to shrink as the particles move inward and in general this motion is rather complex. For example, the particles may spiral around one another along seemingly chaotic orbits. Spectral analysis of the clusters of Fig. 1E reveals a quite different picture in which a new, lower spatial frequency has begun to dominate; this is the frequency of the inter-cluster spacing. The spatial intensity pattern is now characterized by sparseness as the clusters compact and the distances between their edges grow.

For comparison, the simulations were redone by using a fully coherent wavefront as input. In Fig. 2, the spatial intensity pattern at the output is displayed (the simulation parameters correspond to Fig. 1E). As can be seen, the results contrast starkly with those of Fig. 1. Initially, the development is similar to the incoherent case. On top of the featureless beam used as input, MI seeded by noise causes ripples to grow, developing into solitary filaments as the diffractive and nonlinear forces counter each other. After this stage, the two cases are no longer comparable. In the coherent regime, both attractive and repelling forces between the solitary filaments (particles) are present, and we find that the particles will be subject to too many conflicting interactions for any definite course to evolve. Depending on the initial conditions, ordered grid-like patterns may

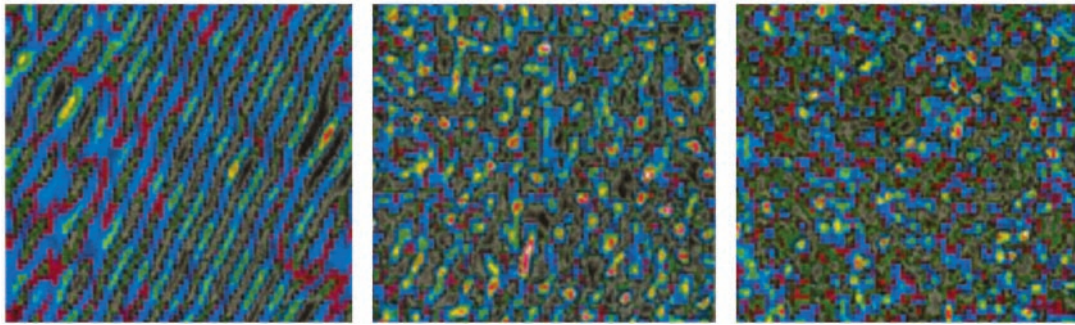


Fig. 3. Experimental results showing pattern development in a biased photorefractive crystal. The coherence length of the beam at the input is $10\ \mu\text{m}$. Shown are the intensity patterns taken at crystal output face (after 10 mm of propagation) for a bias field of 1 kV/cm (Left), 1.8 kV/cm (Center), and 2.6 kV/cm (Right). (Magnifications: $\times 11$.)

form, or the particles may simply remain well spaced apart. In other words, the solitary filaments developing from MI in coherent wavefronts do not cluster. Only when the spatial coherence of the beam is low enough for the long-range repelling forces to disappear can the attractive forces (that survive even when the beam is totally incoherent, that is, the correlation distance is zero) dominate and cause the solitary filaments produced by MI to cluster together.

Our experiments on soliton clustering were performed in a photorefractive nonlinear optical system. A partially spatially incoherent beam was generated by passing an argon ion laser beam ($\lambda = 488\ \text{nm}$) through a rotating diffuser. The spatial coherence of the scattered light from the diffuser was varied by changing the width of the laser beam incident upon the diffuser. The degree of spatial coherence, namely the transverse correlation distance, was monitored by imaging the speckles on the front face of our nonlinear crystal while the diffuser was held stationary. The average speckle size was roughly equal to the transverse correlation distance l_c , representing the longest distance between two points on the transverse plane within which the points are still phase-correlated. A biased strontium barium niobate photorefractive crystal was used as a slow saturable nonlinear medium, with a response time on the order of 10 s. As pointed out in the Introduction, this response time must be much longer than the characteristic random phase fluctuation time created by the rotating diffuser (1 ms in our experiments). The experimental setup was similar to that used in earlier experiments on incoherent MI (49, 56). In our experiments, a broad and uniform extraordinarily polarized optical beam with a controllable degree of spatial coherence was launched into the biased crystal. [The strength of the self-focusing nonlinearity of the crystal was controlled by varying the external bias field and

the intensity of the beam (53–55).] The intensity patterns of the incoherent beam at the crystal output face were monitored by using an imaging lens and a charge-coupled device camera.

Typical experimental results are presented in Fig. 3. These were obtained by using a strontium barium niobate:60 crystal ($5 \times 10 \times 5\ \text{mm}^3$, $r_{33} = 280\ \text{pm/V}$). When the nonlinearity was set to zero (zero bias field), the output beam remained essentially the same uniform broad beam that entered the crystal. As the magnitude of the nonlinearity was increased (by increasing the dc field applied to our nonlinear crystal), the output beam remained uniform until the nonlinearity reached the threshold value for incoherent MI to occur (48, 49). After the threshold nonlinearity, a rather sharp transition in pattern dynamics was observed: the incoherent wavefront disintegrated into one-dimensional stripes at the output (49). Further increases in the nonlinearity led to the appearance of 2D solitary filaments, or particles, with a characteristic width of about $12\ \mu\text{m}$ (similar to the structures observed in ref. 49). To appreciate these solitary filaments, we note that if filaments of this characteristic width are launched in a linear medium they diffract and broaden to at least six times wider after 10 mm of linear propagation (which is the propagation length in our crystal). The self-focusing nonlinearity in our crystal keeps them as nondiffracting solitary light spots, even though the length of our crystal corresponds to roughly five diffraction lengths. Finally, increasing the nonlinearity to even higher levels caused these 2D filaments to cluster together in lumps of fine-scale structures, opening empty voids in other regions upon the beam. The intensity outside the clusters did not drop to zero completely, but clearly more energy was concentrated in the cluster region. This pattern of behavior is in good agreement with our numerical results presented in Fig. 1.

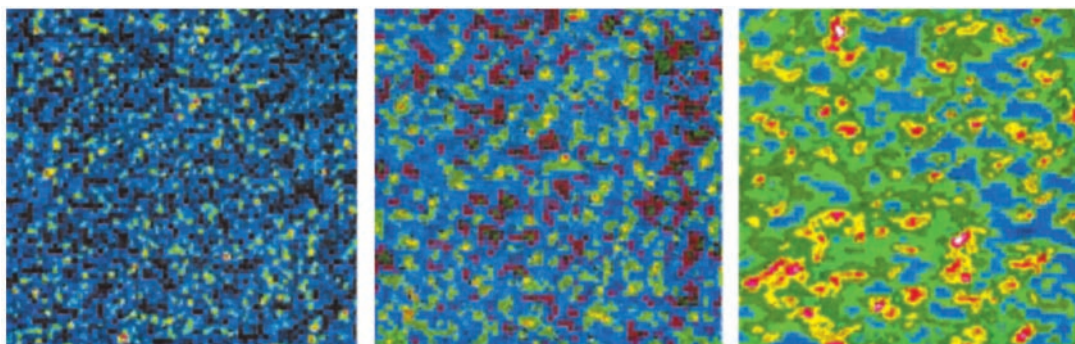


Fig. 4. Experimental results showing pattern development as the coherence of the beam is reduced. The bias field across the crystal is 0.9 kV/cm. Shown are the intensity patterns taken at the output face of the crystal (after 6 mm of propagation) for a coherence length of 6 mm (Left), $30\ \mu\text{m}$ (Center), and $12\ \mu\text{m}$ (Right). The intensity of the last photograph has been enhanced for better visualization. (Magnifications: $\times 11$.)

In addition, we have carried out a series of experiments in different regimes of parameters by varying the nonlinearity saturation and the degree of spatial coherence. In principle, as long as the spatial coherence was below a certain level, repulsion forces between the 2D filaments were practically eliminated on length scales comparable to the correlation length. As a result, forces of an attractive nature dominate the dynamics and clusters of MI filaments form. It seems that the smallest distance between two adjacent fine-scale elements (solitons) in a cluster is determined by the correlation distance: when two filaments become so close that they start to be phase coherent, the repulsive forces will push them apart and prevent them from getting any closer to each other.

The results shown in Fig. 3 depict typical intensity patterns taken from the output face of the crystal at various values of the bias field (keeping all other experimental parameters constant). In this particular experiment, the spatial correlation distance across the beam was roughly $10\ \mu\text{m}$, and the average intensity of the beam at crystal input face was $0.75\ \text{W}/\text{cm}^2$. Similar experiments were performed with different Strontium Barium Niobate crystals under various conditions and correlation distances. Fig. 4 shows experimental results of pattern formation for different degrees of spatial coherence obtained with a Strontium Barium Niobate:75 crystal (6-mm cube, $r_{33} = 870\ \text{pm}/\text{V}$). When the input beam is a spatially coherent wavefront (taken directly from the argon laser without the diffuser), the uniform beam disintegrates as a result of MI, and the resultant filaments tend to form individual well-separated solitons (Fig. 4 *Left*). Even as we increase the nonlinearity further, these soliton filaments still stand on their own and do not merge together. On the other hand, when the beam is made sufficiently incoherent, the correlation between individual filaments becomes insignificant,

and any slight overlapping of their intensity profiles will drag them closer together because of incoherent interaction (50–52). As a result, a broad uniform incoherent beam experiences a global weakly attractive force and tends to form patterns of dense groups of solitary filaments (clusters of 2D solitons). Specifically, in Fig. 4, when the correlation distance is sufficiently reduced to $l_c < 30\ \mu\text{m}$, the onset of soliton clustering occurs (Fig. 4 *Center and Right*). Observing the clustering as a function of decreasing coherence reveals that the peak intensity of individual solitons decreases, and the overall size of soliton clusters increases as more neighboring solitons group together. The size and the shape of each individual cluster as well as the dynamics inside clusters appear to be random and driven by noise.

Conclusion

In summary, we have demonstrated both experimentally and theoretically the spontaneous clustering of solitons in partially coherent wavefronts initiated by random noise. Soliton clustering is an intriguing outcome of the interplay between random noise, weak correlation, and high nonlinearity. Together, these processes lead to incoherent MI, formation of 2D solitary filaments, and eventually to clustering of 2D solitons. Yet all of these fascinating features are not unique to optics. Nonlinear systems involving weakly correlated particles are abundant in nature and so our results may prove relevant to other areas and fields.

This research was supported by the U.S. Army Research Office, Air Force Office of Scientific Research, and the National Science Foundation and is part of the Multi University Research Initiative program on optical spatial solitons. The research at the Technion was supported by the Israeli Ministry of Science, and the research at San Francisco State University was supported by the Research Corporation.

- Bridges, F. G., Hatzes, A. & Lin, D. N. C. (1984) *Nature (London)* **309**, 333–335.
- Bekki, K. (1999) *Astrophys. J.* **510**, L15–L19.
- Spano, F. C. & Mukamel, S. (1991) *Phys. Rev. Lett.* **66**, 1197–1200.
- De Heer, W. A. (1993) *Rev. Mod. Phys.* **65**, 611–676.
- Puls, J., Rabe, M., Winsche, H. J. & Henneberger, F. (1999) *Phys. Rev. B* **60**, R16303–R16306.
- Bratko, D. & Blanch, H. W. (2001) *J. Chem. Phys.* **114**, 561–569.
- Anglin, J. (2000) *Nature (London)* **406**, 29–30.
- O'Dell, D., Giovanazzi, S., Kurizki, G. & Akulin, V. M. (2000) *Phys. Rev. Lett.* **84**, 5687–5690.
- Zakharov, V. E. & Malomed, B. (1994) in *Physical Encyclopedia*, ed. Prokhorov, V. M. (Great Russian Encyclopedia, Moscow), pp. 571–576.
- Lonngren, K. E. (1983) *Plasma Phys.* **25**, 943–982.
- Polturak, E., deVegvar, P. G. N., Zeise, E. K. & Lee, D. M. (1981) *Phys. Rev. Lett.* **46**, 1588–1591.
- Hasegawa, A. & Tappert, F. (1973) *Appl. Phys. Lett.* **23**, 142–144.
- Mollenauer, L. F., Stolen, R. H. & Gordon, J. P. (1980) *Phys. Rev. Lett.* **45**, 1095–1098.
- Askar'yan, G. A. (1962) *Sov. Phys. JETP* **15**, 1088–1090.
- Chiao, R. Y., Garmire, E. & Townes, C. H. (1964) *Phys. Rev. Lett.* **13**, 479–482.
- Bjorkholm, J. E. & Ashkin, A. (1974) *Phys. Rev. Lett.* **32**, 129–132.
- Stegeman, G. I. & Segev, M. (1999) *Science* **286**, 1518–1523.
- Aitchison, J. S., Weiner, A. M., Silberberg, Y., Oliver, M. K., Jackel, J. L., Leaird, D. E., Vogel, E. M. & Smith, P. W. (1990) *Opt. Lett.* **15**, 471–473.
- Kelley, P. L. (1965) *Phys. Rev. Lett.* **15**, 1005–1008.
- Akhmediev, N. N. (1998) *Opt. Quant. Elect.* **30**, 535–569.
- Liu, X., Qian, L. J. & Wise, F. W. (1999) *Phys. Rev. Lett.* **82**, 4631–4634.
- Snyder, A. W., Mitchell, D. J., Polodian, L. & Ladouceur, F. (1991) *Opt. Lett.* **16**, 21–23.
- Mitchell, M., Chen, Z., Shih, M. & Segev, M. (1996) *Phys. Rev. Lett.* **77**, 490–493.
- Mitchell, M. & Segev, M. (1997) *Nature (London)* **387**, 880–883.
- Christodoulides, D. N., Coskun, T. H., Mitchell, M. & Segev, M. (1997) *Phys. Rev. Lett.* **78**, 646–649.
- Christodoulides, D. N., Coskun, T. H., Mitchell, M. & Segev, M. (1998) *Phys. Rev. Lett.* **80**, 2310–2313.
- Mitchell, M., Segev, M., Coskun, T. H. & Christodoulides, D. N. (1997) *Phys. Rev. Lett.* **79**, 4990–4993.
- Mitchell, M., Segev, M., Coskun, T. H. & Christodoulides, D. N. (1998) *Phys. Rev. Lett.* **80**, 5113–5116.
- Snyder, A. W. & Mitchell, D. J. (1998) *Phys. Rev. Lett.* **80**, 1422–1424.
- Shkunov, V. V. & Anderson, D. Z. (1998) *Phys. Rev. Lett.* **81**, 2683–2686.
- Chen, Z., Mitchell, M., Segev, M., Coskun, T. H. & Christodoulides, D. N. (1998) *Science* **280**, 889–892.
- Akhmediev, N., Krolikowski, W. & Snyder, A. W. (1998) *Phys. Rev. Lett.* **81**, 4632–4635.
- Bang, O., Edmundson, D. & Krolikowski, W. (1999) *Phys. Rev. Lett.* **83**, 4740–4743.
- Mitchell, M., Segev, M. & Christodoulides, D. N. (1998) *Phys. Rev. Lett.* **80**, 4657–4660.
- Bespalov, V. I. & Talanov, V. I. (1966) *JETP Lett.* **3**, 307–310.
- Karpman, V. I. (1967) *JETP Lett.* **6**, 277–279.
- Agrawal, G. P. (1987) *Phys. Rev. Lett.* **59**, 880–883.
- Wabnitz, S. (1988) *Phys. Rev. A* **38**, 2018–2021.
- Hasegawa, A. & Brinkman, W. F. (1980) *J. Quant. Elect.* **16**, 694–697.
- Tai, K., Hasegawa, A. & Tomita, A. (1981) *Phys. Rev. Lett.* **56**, 135–138.
- Agrawal, G. P. (1995) in *Nonlinear Fiber Optics* (Academic, San Diego), 2nd Ed., Chapter 5.
- Dianov, E. M., Mamyshv, P. V., Prokhorov, A. M. & Chernikov, S. V. (1989) *Opt. Lett.* **14**, 1008–1010.
- Mamyshv, P. V., Bosshard, C. & Stegeman, G. I. (1994) *J. Opt. Soc. Am. B* **11**, 1254–1260.
- Iturbe-Castillo, M. D., Torres-Cisneros, M., Sanchez-Mondragon, J. & Chavez-Cerda, S. (1995) *Opt. Lett.* **20**, 1853–1855.
- Carvalho, M. I., Singh, S. R. & Christodoulides, D. N. (1996) *Opt. Comm.* **126**, 167–174.
- Zakharov, V. E. & Rubenchik, A. M. (1974) *Sov. Phys. JETP* **38**, 494–500.
- Anastassiou, C., Soljacic, M., Segev, M., Kip, D., Eugenieva, E., Christodoulides, D. N. & Musslimani, Z. H. (2000) *Phys. Rev. Lett.* **85**, 4888–4891.
- Soljacic, M., Segev, M., Coskun, T. H., Christodoulides, D. N. & Vishwanath, A. (2000) *Phys. Rev. Lett.* **84**, 467–470.
- Kip, D., Soljacic, M., Segev, M., Eugenieva, E. & Christodoulides, D. N. (2000) *Science* **290**, 495–498.
- Anderson, D. & Lisak, M. (1985) *Phys. Rev. A* **32**, 2270–2274.
- Shih, M. & Segev, M. (1996) *Opt. Lett.* **21**, 1538–1540.
- Shih, M., Chen, Z., Segev, M., Coskun, T. & Christodoulides, D. N. (1996) *Appl. Phys. Lett.* **69**, 4151–4153.
- Segev, M., Valley, G. C., Crosignani, B., DiPorto, P. & Yariv, A. (1994) *Phys. Rev. Lett.* **73**, 3211–3214.
- Christodoulides, D. N. & Carvalho, M. I. (1995) *J. Opt. Soc. Am. B* **12**, 1628–1633.
- Segev, M., Shih, M. & Valley, G. C. (1996) *J. Opt. Soc. Am. B* **13**, 706–718.
- Klinger, J., Martin, H. & Chen, Z. (2001) *Opt. Lett.* **26**, 271–273.